The College of Engineering
University of Wisconsin-Madison

Wisconsin Electric Machines and Power Electronics Consortium

RESEARCH REPORT
90-2

DESIGN AND CONTROL OF A SERIES RESONANT DC LINK POWER CONVERTER DRIVE

P. Caldeira and T.A. Lipo
Dept. of Elec. and Comp. Eng.
University of Wisconsin-Madison
1415 Johnson Drive
Madison, WI 53706-1691

Y. Murai and S. Mochizuki
Dept. of Electronics & Comp. Eng.
Gifu University
1-1 Yanagido
Gifu, Gifu 501-11, Japan

WEMPEC

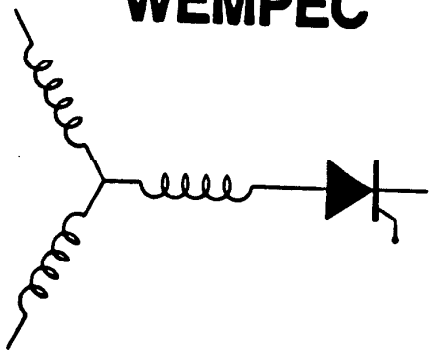

Department of Electrical and Computer Engineering
1415 Johnson Drive
Madison, Wisconsin 53706

Design and Control of a Series Resonant DC Link Power Converter Drive

P. Caldeira and T. A. Lipo
Dept. of Elect & Comp.Eng.
University of Wisconsin-Madison
1415 Johnson Drive
Madison, WI 53706, USA

Y. Murai and S. Mochizuki
Dept. of Electronics & Comp Eng.
Gifu University
1-1 Yanagido
Gifu, Gifu 501-11, Japan

Abstract

In this paper a new control scheme for an induction machine in a high frequency series resonant dc link power conversion system is presented. This system generates a resonant current in a series link and switchings are made at zero current instants, reducing switching losses to a minimal value. Pulse Density Modulation (PDM) strategies utilizing voltage and current regulators control the input and output stages of the resonant system. A field oriented induction machine is utilized as load and unity input power factor operation can be obtained under different load conditions. Overall loss calculation and a design methodology for zero current soft switching schemes are established. Results from digital simulation of the complete ac/ac drive system and its control are presented. Experimental results are obtained from a monophase resonant dc current link prototype.

Introduction

Several types of high power density ac/ac converters utilizing resonant link schemes which use high speed devices have been developed recently. These converters have very low switching losses, since the switching of the devices is made at zero voltage or zero current instants. In general, switching schemes for resonant converters can be classified into ac or dc link modes of operation. The resonant ac circuits utilize a parallel or series resonant link, impressing both polarities of ac voltage and current on the link thus requiring bidirectional switches in the input and output converters[1-3]. Sul and Lipo[4] have investigated a field oriented control and a power flow equalizer for an ac voltage high frequency parallel link power system with an induction machine as load. The resonant dc circuits can also utilize a parallel or series resonant link. Parallel resonant dc link converters have been reported in [5-6].

A high frequency series resonant dc link implemented in an ac-to-ac power converter was proposed in [7] where only 12 unidirectional switches were utilized. As shown in Fig. 1, the capacitor C_0 and inductor L_0 cause a resonant high frequency current i_s to flow from the input ac source to the load while the inductance L_d provides a bias value, I_d, to the resonant current i_s. All thyristors in both the bridges turn on and off at zero current instants, reducing switching losses significantly. However, to minimize problems like current pulse fluctuation and system instability a proportional and derivative current loop feedback and a damping series R-C circuit in parallel with the load were utilized. Introduction of losses and load dependence could be cited as disadvantages for this solution.

A current pulse control strategy for this high frequency resonant link scheme is proposed in [8]. Through proper control of the amplitude of the resonant current pulse delivered to the load, output voltage error can be minimized. A circulating current thyristor is utilized to avoid overexcitation of the capacitors C_0 and C_L. Even though this scheme allows a reduction in the pulse amplitude and voltage stress over the resonant elements, its implementation is fairly complex.

This paper proposes a new control scheme for a field oriented induction machine in an ac/ac drive utilizing the series resonant dc link. Pulse Density Modulation strategy is used on the line/link and link/load converters. A GTO operating in a gate assisted turn-off mode [10] is seen to be a viable option for the switching element. A design methodology for resonant current link schemes based on system loss minimization and component stresses is also established in this paper

A high performance regenerative ac/ac drive system, utilizing a simple PDM strategy, assuring adjustment of the input power factor over a wide range, is proposed for the resonant series link. Fast torque response, small current ripple and an excellent speed regulation in the output stage guarantee a good performance for the field oriented induction machine. Results from digital simulation of the complete system and typical waveforms from a laboratory prototype are presented.

Choice of Switching Device

The resonant dc current link system requires unidirectional current switches which are naturally commutated, since the current pulse drops naturally to zero. Since switching losses are extremely reduced, commutation delays are important parameters to be considered in the selection of the device.

Conventional SCR's would constitute a natural choice for this case but minimum turn-off time requirements would set an upper limit on the switching frequency. Using GTO's in the gate assisted turn-off

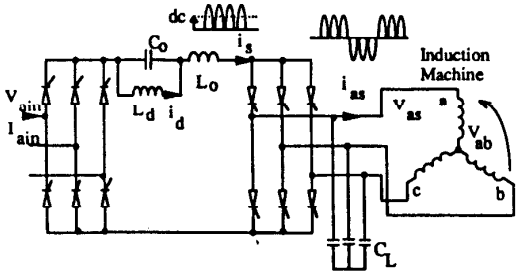

Fig. 1 AC/AC drive system utilizing the series resonant dc link

mode (GATT) was first suggested in [10]. The turn-off process of a GTO in resonant inverters, where the anode current is forced to or naturally reaches zero, approaches that of the SCR. The utilization of the turn-off capability of the GTO in the GATT mode, provides an additional recovery mechanism, thus improving the commutation process efficiency and time. Moreover, small snubbers are required for the whole process.

In an attempt to improve the switching characteristics of a gate assisted turn-off GTO, a series and anti-parallel diodes were incorporated to the basic device in order to avoid the reverse and forward recovery processes reducing significantly the turn-off losses and time [10-11]. Figure 2 shows the GTO being utilized in the gate assisted turn-off mode.

System Analysis

The series resonant link is constituted by the inductor L_0 and capacitor C_0 which resonate at a frequency in a range from 10 to 20 kHz. The resonant current i_s has a sinusoidal waveform and returns to zero after each oscillating period, what guaranties the soft switching procedure. Figure 3 shows a monophase model of the complete ac/ac drive system, where V_o represents the load voltage (line to line motor voltage) and I_d is the dc offset current which is considered constant due to a large value of L_d and to the control strategy of the line/link converter. During one resonant pulse, V_d and V_o are assumed also constants since they are sinusoidal low frequency signals. The resonant current and resonant capacitor voltage can be expressed as

$$i_s(t) = I_d - I_d \cos \omega_0 t + \left(\frac{V_{swt}}{Z_0}\right) \sin \omega_0 t \qquad (1)$$

$$v_c(t) = (V_d - V_o) - I_d Z_0 \sin \omega_0 t - V_{swt} \cos \omega_0 t \qquad (2)$$

where

$$Z_0 = \sqrt{\frac{L_0}{C_0}}, \quad \omega_0 = \frac{1}{\sqrt{L_0 C_0}}, \quad V_{swt} = V_d - V_o - V_{c0}$$

and V_{c0} represents the initial voltage over the resonant capacitor at the beginning of the current pulse. The voltage V_{swt} is the positive voltage required by the switching control to turn on the GTO's.

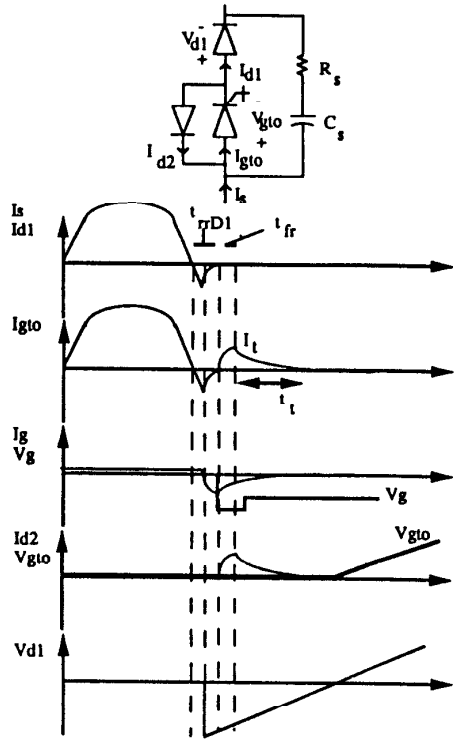

Fig. 2 Turn-off process of a GATT in a series resonant dc link

Figure 4 shows the resonant current $i_S(t)$, voltage over the resonant capacitor and inductor, $v_C(t)$ and $v_l(t)$ respectively, and voltage over the switches $V_{sw}(t)$ during the resonant cycles. During the turn-off process a negative voltage is applied over the switch with a peak value equal to V_{swt}, which constitutes an advantage for the switching turning off process. During the interval between pulses the offset bias current I_d circulates through the resonant capacitor C_0 which discharges linearly from $(V_d - V_o + V_{swt})$ to $(V_d - V_o - V_{swt})$ over a time interval equals to

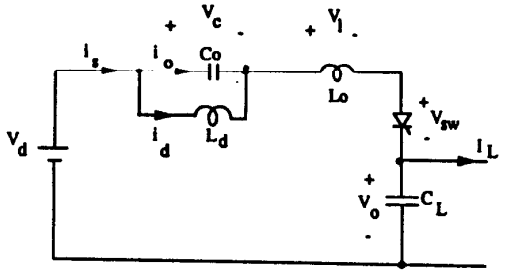

Fig. 3 Monophase model of the ac/ac drive system

$$2\,t_p = 2\frac{V_{swt}\,C_0}{I_d}$$

The resonant period (T_r) can be defined as

$$T_r = T_0 + 2\,t_p$$

where

$$T_0 = \frac{1}{f_0} = \frac{2\pi}{\omega_0} \quad \text{and} \quad T_r = \frac{1}{f_r},$$

The system does not require any special start-up or external excitation circuit since through the application of the adequate positive input voltage V_d, the bias current builds up to its operational value.

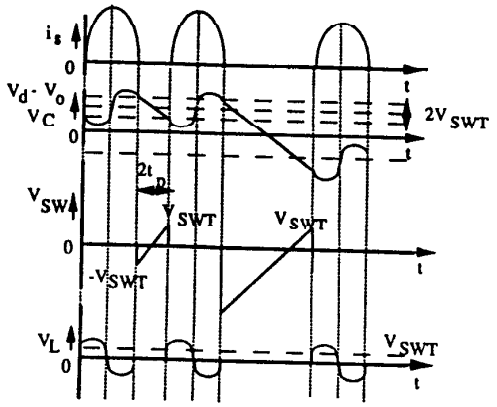

Fig. 4 Waveforms for the monophase resonant dc current link model

Design methodology

A design methodology was presented in [9] for a voltage resonant link system. Loss calculation, device stresses and a component selection procedure for losses minimization is established here for the current link scheme.

A. Device Losses

The main switching devices in a dc current resonant link scheme are subjected to very small losses due to the ideal soft commutation (zero current) conditions.

A.1 Turn-on Loss

At the beginning of the resonant pulse the voltage over the switch falls linearly form V_{swt} to V_{dgto} (device forward drop voltage) during the raise time t_r. The voltage over the GTO can then be expressed as,

$$V_{gto}(t) = \frac{(V_{dgto} - V_{swt})}{t_r}\,t + V_{swt}$$

The voltage over the resonant inductor in this period is

$$v_l(t) = L_0\frac{di_s}{dt} = -\frac{(V_{dgto} - V_{swt})}{t_r}\,t$$

from where the value of i_s can then be calculated as

$$i_s(t) = \frac{(V_{swt} - V_{dgto})}{2\,L_0\,t_r}\,t^2$$

The turn-on loss of one device is

$$P_{on} = \frac{1}{T_r}\int_0^{t_r} V_{gto}(t)\,i_s(t)\,dt$$

hence,

$$P_{on} = \frac{t_r^2}{24\,L_0}\left(V_{swt}^2 - 3V_{dgto}^2 + 2V_{swt}\,V_{dgto}\right) f_r$$

Considering that the slope of the resonant current (di_s/dt) is very low and controllable the turn-on loss is very small.

A.2 Turn-off Loss

During the turn-off process the resonant current falls instantly below zero due to the reverse recovery process of the GTO. Since this device is in series with the fast recovery diode D1, the switch reverse recovery time is very small. When a negative voltage starts to be applied over the main device the anti-parallel diode D2 turns on, avoiding a large reverse voltage over the switch as can be seen in Fig. 2. The turn-off loss is caused by the losses on the reverse recovery (P_{rd} and P_{ra}) and forward reverse recovery process (P_f) and by the loss due to the GTO tail current (P_{tail}).

The negative resonant current circulates during half of the reverse recovery time of the diode D1 (t_{rrD1}) through the GTO. From (1)

$$i_s\left(\frac{t_{rrD1}}{2}\right) = -\left[I_d - I_d\cos\omega_0\frac{t_{rrD1}}{2} + \left(\frac{V_d - V_0 - V_{c0}}{Z_0}\right)\sin\omega_0\frac{t_{rrD1}}{2}\right]$$

Considering the reverse recovery current as linear during t_{rrD1} we have that

$$i_s(t) = 2\,\frac{i_s\left(\frac{t_{rrD1}}{2}\right)}{t_{rrD1}}\,t$$

and

$$P_{rd} = \frac{1}{T_r}\int_0^{\frac{t_{rrD1}}{2}} i_s(t)\,V_{dgto}\,dt$$

The turn- off loss due to the descending reverse recovery process are

$$P_{rd} = \left[i_s(\frac{t_{rrD1}}{2}) \, V_{dgto} \frac{t_{rrD1}}{4} \right] f_r$$

A similar calculation can be done for the ascending recovery process, resulting in

$$P_{ra} = \left[i_s(\frac{t_{rrD1}}{2}) \, V_{dD2} \frac{t_{rrD1}}{4} \right] f_r$$

where V_{dD2} is the forward voltage drop of the diode D2.

Assuming I_t as the peak value that the current i_s can reach during the forward recovery process which last for the time t_{fr}, the forward reverse recovery loss (P_f) is

$$P_f = \left[I_t \, V_{dD2} \frac{t_{fr}}{2} \right] f_r$$

The turn-off loss due to the tail current are calculated considering t_t as the tail current fall time,and a linear decay of the tail current in this time interval. The tail current loss value can be expressed as

$$P_{tail} = \left[I_t \, V_{dD2} \, (\frac{t_t}{2}) \right] f_r$$

It is important to consider that since the main device is switched at zero current and that the diode D2 helps to deplete the gate-cathode junction, the value of I_t is very small, as well as t_t which reduces P_{tail} to a minimum value. Even so, for high frequency operation it becomes an important contribution to the general losses and a main factor for not increasing the switching frequency. The total turn-off loss is

$$P_{off} = P_{rd} + P_{ra} + P_f + P_{tail}$$

A.3 Conduction Loss

The conduction loss of the main device can be calculated as the integral of the product of the resonant current and the GTO forward voltage drop, that is

$$P_{cond} = \frac{1}{T_r} \int_0^{T_0} i_s(t) \, V_{dgto} \, dt$$

giving the following result

$$P_{cond} = V_{dgto} \left[I_d T_0 + \frac{4}{\omega_0} \left(\frac{V_{swt}}{Z_0} - I_d \right) \right] \frac{1}{T_r}$$

The total loss of the main devices, considering that four switches are simultaneously on at the two converters is

$$P_d = 4 \, [P_{on} + P_{rd} + P_{ra} + P_f + P_{tail} + P_{cond}]$$

B. Effect of C_0 ESR and L_d ESR

The losses caused by the resistive element of the resonant capacitor is determined by the current i_s during the resonant pulse and by the bias current I_d

Hence

$$P_{RC0} = P_{RC0p} + P_{RC0d}$$

where

$$P_{RC0p} = \frac{R_{C0}}{2} \left[I_d^2 + \frac{V_{swt}^2}{Z_0^2} \right] \frac{T_0}{T_r}$$

$$P_{RC0d} = I_d^2 \, R_{C0} \left[\frac{2 V_{swt} C_0}{I_d} - T_0 \right] \frac{1}{T_r}$$

The losses caused by the resistive element of the bias inductor is

$$P_{RLd} = I_d^2 \, R_{Ld}$$

The main effect of these resistive components appears in a reduction of the initial voltage of the resonant capacitor in each successive cycle. For larger values of I_d this factor can prevent the application of a negative voltage during the devices turn-off process. This fact could result in a loss of system stability when i_s no longer reaches zero on the next resonant cycle or if the switch could not be turned off due to the immediate positive voltage applied between anode-cathode.

The reduction in V_{swt}, verified since start-up till the regulation stage is reached, is

$$\Delta V_{swt} = n \, (R_{C0} + R_{Ld}) \, I_d$$

where n is the number of resonant pulses in this region. An adequate value of Vswt should be selected to guarantee stable operation for the maximum value of I_d or a correction factor proportional to I_d value can be incorporated over the minimum basic value of V_{swt} necessary for start-up. The second solution seems to have the advantage of minimizing the initial stresses over the system elements.

C. Selection of L_0 and C_0

Considering that
a) the device losses are already reduced
b) capacitors ESR play a minor role on the overall losses
c) losses in L_d depends of its resistive component and of I_d,

the resonant components selection can be made through a minimization of the resonant inductor L_0 losses.

The losses caused by the resistive component (R_{L0}) of the resonant inductor are

$$P_{RL0} = \frac{R_{L0}}{2} \left[3 I_d^2 + \frac{V_{swt}^2}{Z_0^2} \right] \frac{T_0}{T_r} \qquad (3)$$

For an inductor wound with N turns of wire the following relationships are valid

$$L_0 = \frac{1}{R1} N^2 \qquad (4)$$

$$R_{L0} = R2\,N \qquad (5)$$

where R1 and R2 are constants depending on the permeance, cross section area, length and resistivity of the inductance. From equations 4 and 5

$$R_{L0} = R2\sqrt{\frac{Z0\,R1}{\omega 0}} \qquad (6)$$

Substituting this value in P_{RL0} (equation 3) and making its derivative with respect to Z_0, the resultant optimized value for the resonant impedance for minimum losses in the resonant inductor is

$$Z_0 = \frac{V_{swt}}{I_d} \qquad (7)$$

D. Effect of L_0 ESR

The introduction of a resistive element R_{L0} in series with the resonant inductor causes a reduction of the pulse amplitude preventing its return to zero. As in the previous case a reduction in the pulse energy can again result in a loss of system stability since switching at zero current would not take place. The resonant current in this underdamped system can now be solved as

$$i_s(t) = I_d - e^{-\alpha t}\left(I_d \cos\omega_d t + \left(\frac{V_{swt}}{L_0\omega_d} - \frac{\alpha I_d}{\omega_d}\right)\sin\omega_d t\right)$$

where

$$\omega_d = \sqrt{\omega_0^2 - \alpha^2} \text{ and } \alpha = \frac{R_{L0}}{2\,L_0}$$

Considering a linearization of the exponential function and an optimized value of Z_0 for minimum losses in R_{L0} the peak reduction factor (K_r) can be calculated as

$$K_r = \frac{2 + e^{\frac{-\pi R_{L0}}{Z_0}}}{3}$$

E. Selection Criteria for V_{swt}

The positive voltage required by the control to turn-on the main devices (V_{swt}) represents an important parameter on the overall system performance. The points that should be taken into account on the V_{swt} selection criteria are the following

a) V_{swt} must be sufficient large to guarantee the minimum reverse recovery time (t_{rr}) required by the main switch under the zero current turn-off process

b) a variation on the line-neutral input and output voltages from one resonant pulse to another should be taken into consideration

c) since losses are introduced by R_{L0}, the value of V_{swt} should be corrected taking into account the pulse amplitude reduction. Considering the optimized value of Z_0, the correction factor is $1/K_r$.

The selection criteria for V_{swt} can be expressed as

$$V_{swt} \geq \left[\frac{I_d\,t_{rr}}{C_0} + \frac{2\sqrt{3}\pi}{f_r}(V_{inpk}\,f_i + V_{outpk}\,f_o)\right]\frac{1}{K_r}$$

where f_i and f_o are the input and output voltage frequencies.

F. Voltage and Current Stresses - I_s, V_c, V_{sw}, V_l

If equation 1 and 2 are squared and added, equation 8 is obtained, which represents a phase plane plot of the resonant current, i_s, and resonant capacitor voltage, v_c, during start up and normal operation of the system as can be seen in Fig.5.

$$(i_s(t) - I_d)^2 + \left(\frac{v_c(t)}{Z_0} - \frac{(V_d - V_0)}{Z_0}\right)^2 = I_d^2 + \left(\frac{V_d - V_0 - V_{c0}}{Z_0}\right)^2 \qquad (8)$$

From the system phase plane plot the maximum values of i_s and v_c can be calculated as

$$i_{speak} = I_d + \sqrt{I_d^2 + \left(\frac{V_{swt}}{Z_0}\right)^2}$$

$$v_{cpeak} = (V_d - V_0) + Z_0\sqrt{I_d^2 + \left(\frac{V_{swt}}{Z_0}\right)^2}$$

Considering that the input and output voltage can assume any possible combination depending on the modulation strategy, the maximum variation of the resonant capacitor voltage would be

$$\Delta v_{cmax} = 2\,(V_d + V_0) + 2\,Z_0\sqrt{I_d^2 + \left(\frac{V_{swt}}{Z_0}\right)^2}$$

where V_d and V_0 are the maximum positive voltages

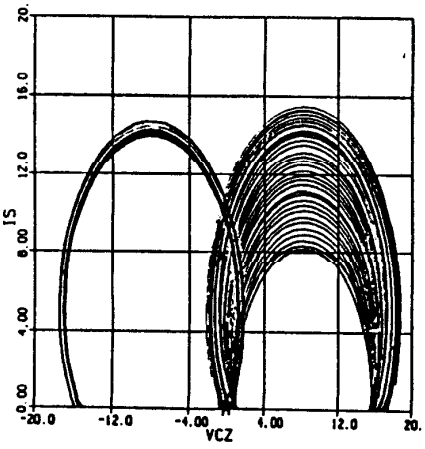

Fig. 5 Phase plane plot of i_s and v_c

applied in both sides of the link (output voltages of the line/link and link/load converters respectively). The maximum voltage stress over the input or output switches are

$$V_{swmax} = \sqrt{3}[V_{pk} - 2(V_{inpk} + V_{outpk})] - V_{swt}$$

where V_{pk} represents the input or output line-neutral peak voltage respectively. It should be noticed that the voltage stress over the main switches (GTO's)is practically zero, considering the action of the series and anti-parallel diodes on the switch arrangement utilized.

The peak voltage over the resonant inductor L_0 is

$$V_{Lpk} = Z_0 \sqrt{I_d^2 + \left(\frac{V_{swt}}{Z_0}\right)^2}$$

Overall System Control

A. Line/Link Converter Control

The average value of the resonant current i_s is approximately the value of the bias current. A regulation control for the current I_d is then necessary to guarantee zero crossing switching instants. If large variations in I_d occurs the current pulses i_s no longer reach zero, which would not allow the intended zero current switching procedure for this type of system. Through an adequate switching sequence of the input converter the desired voltage V_d is applied to the link in an effort to equalize the value of the current I_d to a set value (I_{dref}).

Changes in load determine a variation in the output voltage. Since the resonant pulse amplitude depends on the input and output voltages and link capacitor initial voltage, its average value, I_d, changes. In this way instantaneous power variation results in a link current fluctuation and a correction signal from the I_d error is generated. A sigma delta modulator is employed for this purpose.

A second correction signal is provided by an average power loop. The power balance equation for this system can be written as:

$$P_{IN} + \frac{d}{dt}\left(\frac{1}{2} \cdot L_d \cdot I_d^2\right) + P_{OUT} = 0$$

where P_{IN} and P_{OUT} represents the input and output power respectively. To obtain the average power information, instantaneous power can be measured from the induction machine utilized as load and integrated through a low pass filter. This signal is compared with the input power and the necessary input current amplitude is obtained as shown in Fig. 6. These two correction signals from the I_d regulation loop and power loop are added and the final input reference current amplitude I_{in} is generated. Since a three phase sigma delta current regulator is utilized, I_{in} is transformed into a three phase sinusoidal current reference signal in phase with the input voltages, if a unity input power factor operation is desired.

The current references I_{ainref}, I_{binref} and I_{cinref} are compared with the actual input currents and the generated errors determine the phases to be triggered in the input converter. The sum of these three errors must satisfy the relation

$$\varepsilon_{ain} + \varepsilon_{bin} + \varepsilon_{cin} = 0$$

from which the triggering principle can be established based on the fact that the three errors can never have the same polarity. The triggering principle is,

a) the thyristor in the phase having the larger error out of the two phases of the same polarity is chosen to be triggered
b) the phase corresponding to the error with the opposite polarity error is selected as the other triggering phase.

Instantaneous power matching control is not possible, but average power matching can be achieved, resulting in a minimization of the variations in the I_d current, helping to accomplish the two main objectives of this control scheme which are regulation of the bias current I_d and unity input power factor. The average power loop is not necessary for the system operation, since power matching is automatically obtained through I_d regulation. Although, the utilization of this loop speeds the system response to load variation and avoids overexcitation of the I_d regulator.

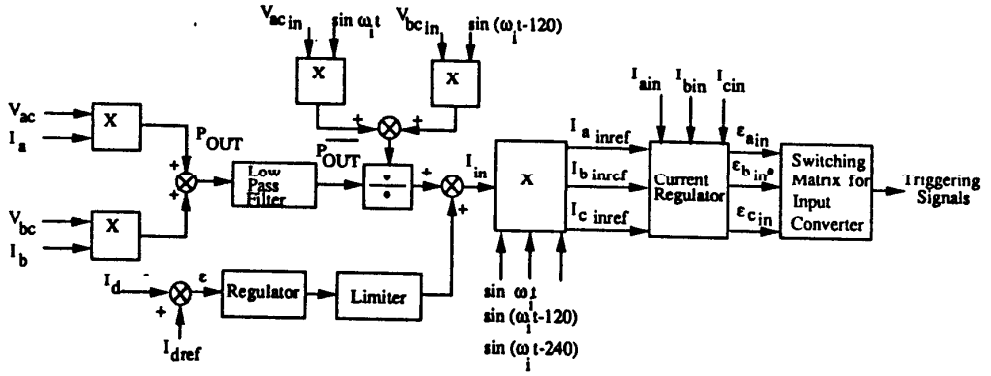

Fig.6 Id regulator and unity power factor controller

B. Link/load Converter Control

For the output signal control an internal load voltage feedback loop in the ABC reference frame and an external load current feedback loop in the synchronous DQN reference frame are utilized, as shown in Fig. 7. Area Comparison Pulse Density Modulation regulators [1] are responsible for the distribution of the resonant pulses among the three output lines. The internal loop utilizes a voltage regulator where the load voltage is compared with three reference voltage signal generated from the errors of the current regulator on the external control loop.

The current regulator compares the load current in the DQN reference frame (i_{qs} and i_{ds}) with a torque and flux command generated by an outer speed loop control. The speed regulator and torque limiter generate the torque command, which corresponds to the q-component of the reference current. The flux command is determined by the d-component of the reference current. The reference slip angular velocity is then calculated in a slip calculator accordingly to the following equations

$$s\omega_e = \frac{r_r L_m}{L_r} \frac{i^e_{qsref}}{\lambda^e_{dr}}$$

and

$$\lambda^e_{dr} = \frac{r_r L_m}{r_r + L_r p} i^e_{dsref}$$

where "p" represents the derivative operator, λ^e_{dr} is the d axis component of the rotor flux, and r_r, L_m, L_r are the rotor resistance, magnetizing and rotor inductance (magnetizing and leakage) respectively.

The reference slip is integrated and summed with the rotor position angle to form the field angle θ_e that is used in the two coordinate conversion processes between the reference frames, assuring a field oriented operation for the induction machine.

Simulation Results

Figure 8 shows output voltage and current, input voltage and fundamental current, transient torque response, motor speed and motor flux under load variation obtained from digital simulation. No system instability was observed over numerous different operational conditions. A 7.5 Hp, 230V , 60Hz was utilized in the simulation.

Experimental Results

A monophase model of the resonant dc current link system, has been assembled in laboratory. The control algorithm described above was implemented utilizing a DSP Motorola 56000 system. Figure 9-a shows a complete operational cycle (charging, regulation and discharging modes) of the circuit. No special devices or procedure are necessary for start-up. With the adequate selection of V_{swt} no excitation circuits needed to be employed. The maximum resonant frequency obtained was approximately 17kHz with a maximum value of 25 A for the bias current I_d. A detailed view of the resonant pulse and the voltage over the switch is shown in Fig. 9-b.

A proportional correcting signal for detecting i_s zero crossings for different values of I_d was implemented, assuring zero current switching for different load conditions. Another proportional correcting signal is also responsible for the variation of V_{swt} with the goal to maintain complete system stability under any operating condition. Special GTO drivers have been designed and constructed for high frequency switching. A three phase version of the system is currently being implemented. The System parameters are:

$C_0 = 1\mu F$, $L_0 = 185\mu F$, $L_d = 80mH$, $V_d = 110V$, $V_{swt\ min} = 50V$

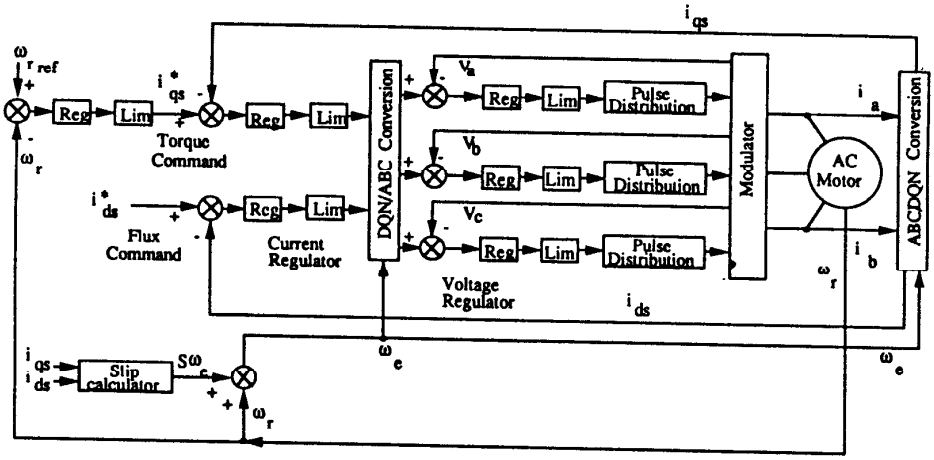

Fig.7 Field oriented scheme for an induction machine in a series resonant link system

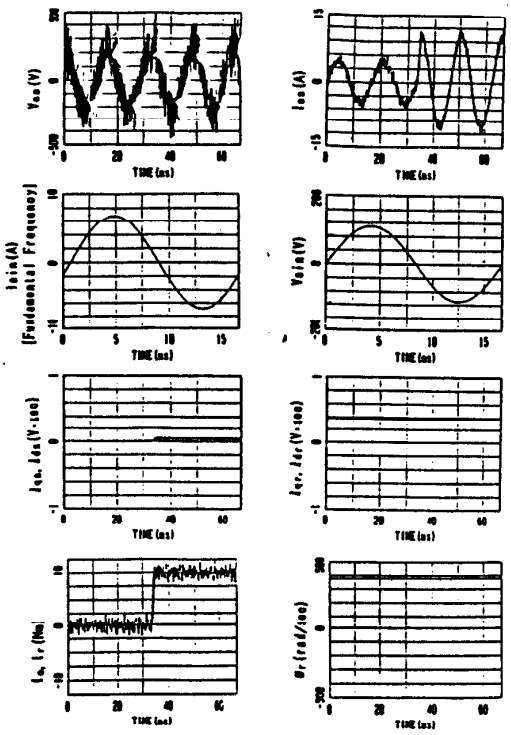

Fig. 8 Simulated waveforms for the series resonant dc link drive

Conclusion

A new control scheme for an induction machine in a high frequency series resonant dc link system is presented. Pulse Density Modulated converters distributed the resonant pulses in the input and output ac lines and unity input power factor operation can be obtained under different load conditions. A design methodology for the dc current link schemes, taking into consideration the overall losses in the system and component stresses was established and utilized in the implementation of a laboratory prototype.

A digital simulation of the complete control strategy was performed and demonstrated the overall performance of the system. Fast torque response, low output ripple, absence of instability under load variation, simple structure can be seen as advantages of the proposed control. High voltage stress over switches and resonant elements constitute disadvantages of the topology. Experimental results performed on a monophase model demonstrate the validity of the analytical model studied.

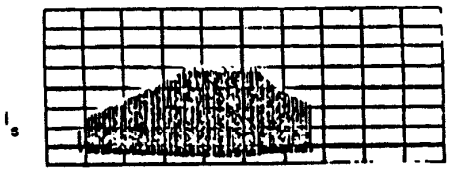

(a) Complete operational cycle

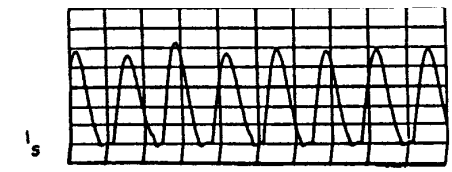

(b) Detail of the resonant pulse

Fig. 9 Experimental results of the monophase model

References

[1] P. Sood and T. A. Lipo, "Power Conversion Distribution System Using a Resonant High Frequency AC Link", IEEE-IAS Annual Meeting Conference Record, 1986, pp. 533-541.

[2] H. K. Lauw, J. B. Klaassens, N. G. Butler and D. B. Seely, "Variable-Speed Generation with the Series-Resonant Converter", IEEE-PES Winter Meeting Conference Record, 1987/1988.

[3] S. W. H. de Haan and J. D. Lodder, "A Formalistic Approach to Series-Resonant Power Conversion", EPE Conference Record, 1987, pp. 231-238.

[4] Seung K. Sul and T. A. Lipo,"Field Orientation Control of an Induction Machine in a High Frequency Link Power System", PESC Conference Record, 1988, pp. 1084-1090.

[5] D. M. Divan, "The Resonant DC Link Converter--A New Concept in Static Power Conversion", IEEE IAS Annual Meeting Conference Record, 1986, pp. 648-656.

[6] D. M. Divan and G. L. Skibinski, "Zero Switching Loss Inverters for High Power Applications", IEEE IAS Annual Meeting Conference Record, 1987, pp. 627-634.

[7] Y. Murai and T. A. Lipo, "High Frequency Series Resonant DC Link Power Conversion", IEEE IAS Annual Meeting Conference Record, 1988, pp. 772-779.

[8] Y. Murai, S. Mochizuki, P. Caldeira, T. A. Lipo, "Current Pulse Control of High Frequency Series Resonant DC Link Power Converter", IEEE IAS Annual Meeting Conference Record, 1989, pp. 1023-1030,.

[9] D. M. Divan , G. Venkataramanan and R. DeDoncker, "Design Methodologies for Soft Switched Converters", IEEE-IAS Conference Records Annual Meeting, 1988, pp. 758-766.

[10] S. M. Tenconi and M. Zambelli, "The Reverse Blocking GTO as a Very Fast Turn- Off Thyristor", IEEE IAS Conference Records Annual Meeting, 1986, pp. 377-383.

[11] L. Malesani, L. Rossette and P. Tenti, "50 kW, 30kHz GTO Inverter for Induction Heating Applications", UEI Workshop on Induction Heating and Melting, Hannover, 1988,pp. 105-109.